MACEIÓ - ALAGOAS
EBA 15
15° ENCONTRO BRASILEIRO SOBRE ADSORÇÃO
15th Brazilian Meeting about Adsorption

Fixed bed adsorption of Pb^{2+} by an agar-graphene oxide hydrogel

N. B. V. Serafim [a], C. M. B. Araujo [b], J. V. F. L. Cavalcanti [a], M. A. Motta Sobrinho [a], A.F. P. Ferreira [c]

[a] *Federal University of Pernambuco, Chemical Engineering Department, 50670-901 Recife, Brazil*
[b] *University of Minho, R. da Universidade, 4710-057 Braga, Portugal*
[c] *University of Porto, Faculty of Engineering, Department of Chemical Engineering, 4200-465 Porto, Portugal*

Abstract

Heavy metals are predominantly introduced into the environment through industrial waste. To address this issue, graphene-based nanomaterials incorporated into polymeric matrices present a promising solution for effective adsorption and reuse in treating contaminated wastewaters. This study investigates the use of a hydrogel composed of agar and graphene oxide for the removal of Pb^{2+} ions from aqueous solutions in a fixed-bed system. The hydrogel demonstrated high recovery percentages over three adsorption-desorption cycles. Breakthrough times aligned with model predictions, and the uptake capacity closely matched results from previous batch tests. These findings suggest that the graphene oxide-agar hydrogel is an effective adsorbent for removing Pb^{2+} ions from aqueous solutions.

Keywords: adsorption; agar; graphene oxide; heavy metal; fixed bed.

1. Introduction

Heavy metals are toxic substances that pose significant health risks, predominantly introduced into the environment through the discharge of untreated or inadequately treated industrial waste [1][2]. To mitigate the concentration of these harmful substances in the environment, adsorption has become one of the most extensively studied processes for the post-treatment of effluents contaminated with heavy metals [3]. As a result, much scientific effort focuses on developing efficient adsorbent materials [4]. In this context, graphene-based nanomaterials have gained considerable attention due to their remarkable properties, such as high surface area and chemical stability [5].

However, the nanoscale nature of graphene-based materials presents challenges for industrial applications, particularly in separating them after use. Incorporating these materials into polymer matrices offers a practical solution, combining their advantageous properties with the structural benefits of the matrix [6]. This method allows for the creation of adsorption beds that can be reused through multiple adsorption-desorption cycles [7]. This study explores the use of a nanocomposite composed of graphene oxide and agar in a fixed bed system for the removal of Pb^{2+} ions from aqueous solutions.

2. Experimental

The experiments were carried out using the setup illustrated in Fig. 1. A stainless-steal column, 10 cm in height and 2 cm in internal diameter, was packed with a hydrogel composite of agar and graphene oxide (GO). An aqueous Pb^{2+} solution was pumped upwards through the column at 25ºC. Samples were periodically collected from the top of the column, and the Pb^{2+} concentration was analyzed using ICP-OES. Flow rates of 2 $mL \cdot min^{-1}$ and 4 $mL \cdot min^{-1}$ were employed and regularly monitored to maintain consistency. After the adsorption phase, the column was treated with a 0.1 $mol \cdot L^{-1}$ HCl solution for desorption, followed by water util a pH of 7 was achieved. Table 1 shows some data from adsorbent characterization [8].

The bed porosity and Peclet number were determined using blue dextran tracer test, the experiment was conducted in the same conditions of fixed bed experiments. The tests were carried out in duplicate, the passage time of the tracer through the column is 6 min. The Peclet number was then used to estimate axial dispersion according to Eq. 1. Table 2 presents the parameters for the fixed bed breakthrough experiments.

$$Pe = \frac{v_i H}{D_{ax}} \quad (1)$$

Table 1. Data from adsorbent characterization

Parameter	Value
Pores volumn ($cm^3 \cdot g^{-1}$)	7.8×10^{-4}
Pores diameter (nm)	1.1
Zeta potential	2.0

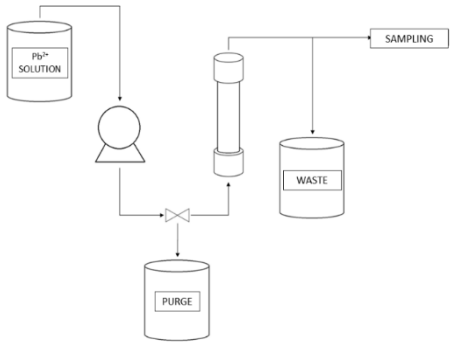

Fig. 1. Setup of the fixed-bed column experiment for continuous Pb^{2+} ion adsorption.

Table 2. Parameters for the fixed bed experiments.

Parameter	Value
Height of the bed (H_b, m)	0.10
Internal diameter of the column (d_i, m)	0.02
Adsorbent mass (m_{bed}, $g_{drv\ adsorbent}$)	0.336
Bulk porosity (ε_b)	0.40
Peclet number (Pe)	11.66
Coefficient of axial dispersion (D_{ax}, $m^2 \cdot min^{-1}$)	1.36×10^{-4}
Particle size (d_p, mm)	2.2
Flow rate (Q, $mL \cdot min^{-1}$)	2.00
Interstitial velocity (v_i, $m \cdot min^{-1}$)	0.016
Pb^{2+} feed concentration (C_0, $mg \cdot L^{-1}$)	20.0
Intraparticule mass transfer coefficient (k_{LDF}, min^{-1})	0.038
Freundlich index (n, dimensionless)	2.0
Freundlich constant (K_f, $mg \cdot L^{1/n-1}$)	12.1

From the experimental data, it was possible to estimate the breakthrough time (C_t = 0.05 C_0), stoichiometric time, and exhaustion time (C_t = 0.95 C_0), as well as the uptake capacity (Eq. 3.).

$$t_{st} = \int_0^{\infty} \left(1 - \frac{C}{C_{\infty}}\right) dt \quad (2)$$

$$q_e = \frac{C_{\infty} \cdot Q \cdot t_{st} - \varepsilon_b \cdot V \cdot C_{\infty}}{m} \quad (3)$$

To predict the breakthrough behavior, a computational simulation was employed, using experimental parameters listed in Table 2, achieved by solving Eq. 4.

$$D_{ax} \frac{\partial^2 C}{\partial z^2} - v_i \frac{\partial C}{\partial z} - \frac{\partial C}{\partial t} - \frac{1-\varepsilon}{\varepsilon} \frac{\partial q}{\partial t} = 0 \quad (4)$$

Assuming that initial condition is: $t = 0 \rightarrow C_0 = q_0 = 0$ and boundary conditions are: $z = H \rightarrow \partial C/\partial z = 0$ and $z = 0 \rightarrow D_{ax}\ \partial C/\partial z = v_i(C - C_{\infty})$.

3. Results and discussion

The results for the breakthrough curves from three fixed-bed cycles with flow rates of 2 $mL \cdot min^{-1}$ (Fig. 2) and 4 $mL \cdot min^{-1}$ (Fig. 3) are presented. The adsorption curves exhibit a symmetric "S" shape. Desorption of Pb^{2+} ions with 0.1 $mol \cdot L^{-1}$ HCl required 60 minutes for both flow rates. The percentage recovery of Pb^{2+} ions is shown in Table 3.

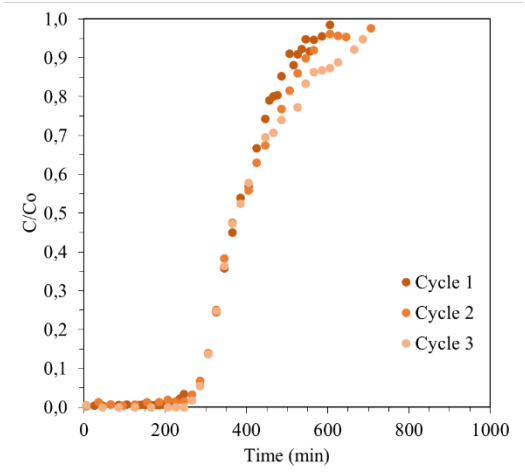

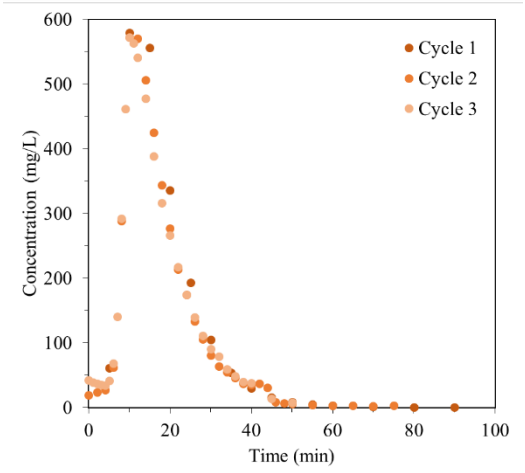

Fig. 2. Breakthrough curves for Pb^{2+} ion adsorption (a) and desorption (b) using the composite hydrogel at a flow rate of 2 mL·min^{-1}.

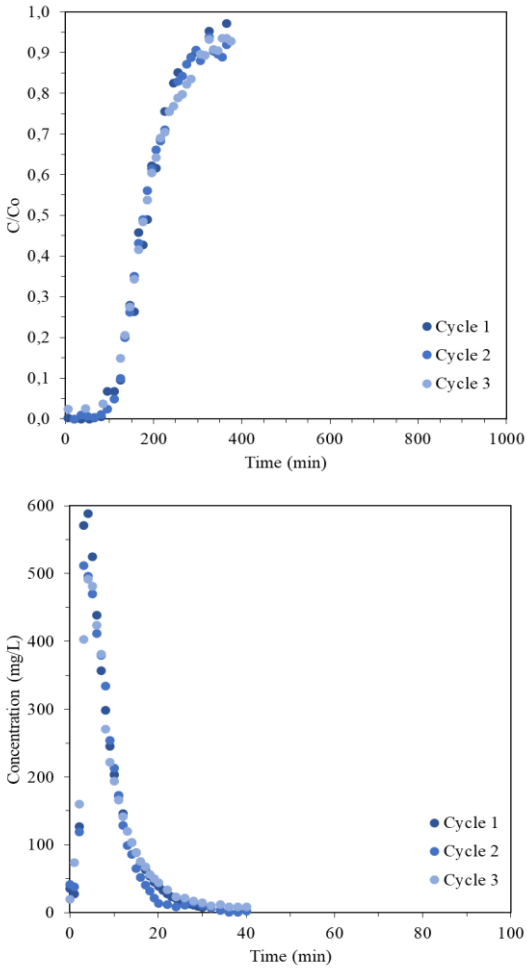

Fig. 3. Breakthrough curves for Pb^{2+} ion adsorption (a) and desorption (b) using the composite hydrogel at a flow rate of 4 mL·min^{-1}.

Table 3. Percentage recovery of Pb^{2+} ions through cycles using 0.1 mol·L^{-1} HCl as the eluent.

Cycle	2.0 mL·min^{-1}	4.0 mL·min^{-1}
1	95.6%	97.9%
2	94.4%	86.1%
3	89.5%	86.6%

Comparing the flow rates, a higher percentage recovery was achieved at 2 mL·min^{-1}. This is likely due to the increased contact time between the phases. Since the breakthrough curves for the three cycles are quite similar, the data were combined to create a single curve, presented in Fig. 4, alongside the prediction curve from the computational simulation.

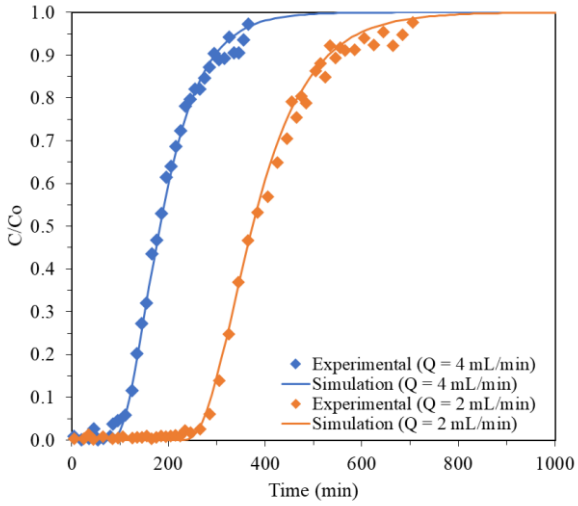

Fig. 4. Combined breakthrough curves for Pb^{2+} ion adsorption on the composite hydrogel at two different flow rates, along with the predicted curve from the computational simulation.

The breakthrough time was estimated 274 min for the 2 mL·min^{-1} flow rate and 104 min for the 4 mL·min^{-1} flow rate. The exhaustion time was 674 min for 2 mL·min^{-1} and 370 min for 4 mL·min^{-1}. The higher flow rate resulted in faster breakthrough and exhaustion times. By increasing the flowrate, if the system is under internal mass transfer resistance (which seems to be the case here), when the contact time between the adsorbate and the adsorbent decreases, the breakthrough time also decreases [9].

The experimental data closely match the predictions from the computational simulation, with the prediction errors detailed in Table 4.

Table 4. Prediction errors from the computational simulation for Pb^{2+} ion adsorption in the composite hydrogel.

Flowrate (mL·min^{-1})	2.0	4.0
Mean absolute error (MAE)	0.02	0.02
Mean squared error (MSE)	0.0006	0.0007
Root meat squared error (RMSE)	0.02	0.03

Figures in Fig. 4 and the errors in Table 4 indicate that the experimental data align closely with the predicted model, showing minimal deviation. Table 5 presents the adsorptive capacities from the fixed-bed tests and those predicted by fitting the

Freundlich isotherm to equilibrium data for Pb^{2+} adsorption on the composite hydrogel in batch tests. As it could be seen, the error between the batch adsorption capacity and those estimated from fixed-ben tests were below 12%.

Table 5. Adsorptive capacities obtained on a dry basis from fixed-bed tests compared with the predicted values from Freundlich's isotherm.

	q ($mg \cdot g^{-1}$)	Relative error (%)
Freundlich (Batch tests)	50.53	-
Fixed-bed (2 $mL \cdot min^{-1}$)	44.67	11.60
Fixed-bed (4 $mL \cdot min^{-1}$)	46.30	8.37

This composite hydrogel demonstrates superior performance compared to steam granular activated carbon packed in a fixed bed of similar dimensions (10 cm x 1.5 cm). The carbon achieved an uptake capacity of 0.123 $mg \cdot g^{-1}$, while the hydrogel reached 46.3 $mg \cdot g^{-1}$ at the same flow rate, on a dry basis [10].

4. Conclusions

In this study, the performance of a hydrogel composite based on graphene oxide and agar in a fixed bed system for Pb^{2+} ion adsorption was evaluated. The hydrogel demonstrated effective recovery across three adsorption-desorption cycles. The breakthrough times aligned well with model predictions, and the uptake capacity closely matched the values obtained from batch tests. These findings indicate that the graphene oxide-agar hydrogel is a highly efficient adsorbent for the removal of Pb^{2+} ions from aqueous solutions.

Acknowledgements

The authors acknowledge the financial support provided by the Coordenação de Aperfeiçoamento de Pessoal de Nível Superior – Brasil (CAPES) – Finance Code 001, Conselho Nacional de Desenvolvimento Científico e Tecnológico (CNPq, grant/award number: 401905/2022-5), Fundação de Amparo à Ciência e Tecnologia do Estado de Pernambuco (FACEPE) (IBPG-1860-3.06/21) and this work was partially supported by national funds through FCT/MCTES (PIDDAC): LSRE-LCM, UIDB/50020/2020 (DOI: 10.54499/UIDB/50020/2020) and UIDP/50020/2020 (DOI: 10.54499/UIDP/50020/2020); and ALiCE, LA/P/0045/2020 (DOI: 10.54499/LA/P/0045/2020).

References

[1] Vardhan KH, Kumar PS, Panda RC. A review on heavy metal pollution, toxicity and remedial measures: Current trends and future perspectives. Journal of Molecular Liquids, v. 290, p. 111197, 2019.
[2] Zhou Q, Yang N, Li Y, Ren B, Ding X, Bian H, Yao X. Total concentrations and sources of heavy metal pollution in global river and lake water bodies from 1972 to 2017. Global Ecology and Conservation, v. 22, p. e00925, 2020.
[3] Fei Y, Hu YH. Recent progress in removal of heavy metals from wastewater: A comprehensive review. Chemosphere, p. 139077, 2023.
[4] Chai WS, Jie YC, Kumar PS, Mubashir M, Majeed Z, Banat F, Ho S, Show PL. A review on conventional and novel materials towards heavy metal adsorption in wastewater treatment application. Journal of Cleaner Production, v. 296, p. 126589, 2021.
[5] Joshi NC, Gururani P. Advances of graphene oxide based nanocomposite materials in the treatment of wastewater containing heavy metal ions and dyes. Current Research in Green and Sustainable Chemistry, v. 5, p. 100306, 2022.
[6] Hassan MS, Bai J, Dou D. Biopolymers; definition, classification and applications. Egyptian Journal of Chemistry, v. 62, n. 9, p. 1725-1737, 2019.
[7] Khan ZU, Khan WU, Ullah B, Ali W, Ahmad B, Ali W, Yap P. Graphene oxide/PVC composite papers functionalized with p-Phenylenediamine as high-performance sorbent for the removal of heavy metal ions. Journal of Environmental Chemical Engineering, v. 9, n. 5, p. 105916, 2021.
[8] Araujo CMB, Wernke G, Ghislandi MG, Diório A, Vieira MF, Bergamasco R, Motta Sobrinho MA, Rodrigues AE. Continuous removal of pharmaceutical drug chloroquine and Safranin-O dye from water using agar-graphene oxide hydrogel: Selective adsorption in batch and fixed-bed experiments. Environmental Research, v. 216, p. 114425, 2023.
[9] Dotto GL, Santos JMN, Rosa R, Pinto LAA, Pavan FA, Lima EC. Fixed bed adsorption of Methylene Blue by ultrasonic surface modified chitin supported on sand. Chemical Engineering Research and Design, v. 100, p. 302-310, 2015.
[10] Meshram S, Dharmadhikari S, Raghwendra ST, Soni AB, Thakur C. Fixed-bed adsorption of lead from battery recycling unit wastewater-optimization using Box-Behnken method. Journal of Hazardous Materials Advances, v. 10, p. 100297, 2023.